processes

MDPI

Article

Computational Study of the Adsorption of Phosphates as Wastewater Pollutant Molecules on Faujasites

Luis Fernando Capa-Cobos, Ximena Jaramillo-Fierro and Silvia González *

Departamento de Química, Facultad de Ciencias Exactas y Naturales, Universidad Técnica Particular de Loja, Loja 11-01-608, Ecuador; lfcapa@utpl.edu.ec (L.F.C.-C.); xvjaramillo@utpl.edu.ec (X.J.-F.)
* Correspondence: sgonzalez@utpl.edu.ec

Abstract: The adsorption of sodium dihydrogen phosphate (NaH_2PO_4) onto X- and Y-type faujasite zeolites was computationally studied using the Density Functional Theory (DFT) method. The structures were modeled using the Materials Studio software. The Si/Al ratios for the X- and Y-type zeolite models were 1.2 and 2.5, respectively. The central pore of the zeolite provided a more favorable coordination for adsorbing NaH_2PO_4. Full molecular optimization and adsorption energy calculations were performed using the VASP code. The adsorption was more effective on zeolite Y, with an adsorption energy of 161 kJ/mol, compared to the zeolite X system, with an adsorption energy of 31.64 kJ/mol. This calculated value for X-type faujasite was found in the interval of the adsorption energy of $H_2PO_4^-$ on hydrated Fe oxide (94.4 kJ/mol) and modified polyether sulfone (22.5 kJ/mol), and the calculated adsorption energy of the molecule on Y-type faujasite coincides with the reported value for this adsorbate on Mg/Ca-modified biochar structures. The molecular conformations of the adsorbate on the two studied models are very different, so the difference between the adsorption energy values of each type of zeolite model is comprehensible. On the one hand, the oxygen atoms of the molecule formed a bidentate complex with the hydrogen atoms of the pore in the X-type faujasite model, and the O-H distance was 1.5 Å. On the other hand, an adsorbed oxygen atom of the phosphate was placed on a hydrogen atom at site II of the Y-type faujasite zeolite, and two of the hydrogen atoms of the phosphate were placed on the oxygen atoms. The Bader analysis results indicated that the negative charge of the phosphate anions was delocalized on the zeolites protons. The hydroxy groups of the phosphate form bonds between their hydrogen atoms and the oxygen atoms of the zeolite porous structure; therefore, we concluded that these sites have an alkaline character. The aim of this study was to include a computational analysis of possible phosphate adsorption mechanisms in faujasite zeolites that can be confirmed by experimental tests, and hence contribute to the generation of new technologies for capturing pollutant molecules in wastewater. The results are in agreement with the experimental information concerning the influence of pH on the adsorption activity of phosphate adsorption on zeolites.

Keywords: faujasite; phosphate; adsorption; DFT; wastewater treatment

check for updates

Citation: Capa-Cobos, L.F.; Jaramillo-Fierro, X.; González, S. Computational Study of the Adsorption of Phosphates as Wastewater Pollutant Molecules on Faujasites. *Processes* **2021**, *9*, 1821. https://doi.org/10.3390/pr9101821

Academic Editor: Andrea Melchior

Received: 14 September 2021
Accepted: 7 October 2021
Published: 14 October 2021

Publisher's Note: MDPI stays neutral with regard to jurisdictional claims in published maps and institutional affiliations.

Copyright: © 2021 by the authors. Licensee MDPI, Basel, Switzerland. This article is an open access article distributed under the terms and conditions of the Creative Commons Attribution (CC BY) license (https://creativecommons.org/licenses/by/4.0/).

1. Introduction

Phosphorus is a mineral nutrient that is essential for all living species; however, its excessive concentration when dissolved in natural water sources, which is caused by untreated waste from agricultural, domestic, and industrial sources, causes eutrophication problems [1–5]. Common phosphate species with natural pH conditions are $H_2PO_4^-$ and HPO_4^{2-} [6].

Recently, the need to remove phosphate from water has become a hot research topic, and a variety of methods have been developed, mainly involving biological, physical, and chemical treatments [7,8]. The disadvantages of traditional treatments are their low selectivity towards phosphate over competing anions and other dissolved organic compounds, their low adsorption capacity in the neutral pH range, the deactivation of their adsorption capacity, and their ineffective regeneration [9–11].

Due to their high specific surface area, adsorption capacity, catalytic removal activity, abundance, availability, and low cost, the use of zeolites such as faujasite X (FAU-X) and faujasite Y (FAU-Y) is a feasible option in wastewater treatment due to their superior properties compared to those of sand or carbon filters [12–15]. These zeolites are formed by a three-dimensional Al_2O_4 and SiO_4 tetrahedral lattice that shares oxygen atoms [16]. In this lattice, the negative charge is caused by the isomorphic substitution of Si^{4+} by Al^{3+}, and compensated by additional cations, such as H^+ protons, to form Brønsted acid sites in the zeolites [17].

The crystal structure of faujasite-type zeolites is the Fd3m symmetry space group. Their structure is composed of sodalite cages (also called β-cages), with a diameter of 6.6 Å. These units are interconnected by a hexagonal prism with a basis of 2.3 Å (D6R). The sodalite cages are connected to supercages (also called α-cages) by other windows, with a diameter of 12.4 Å. Finally, these supercages are linked together by a hexagonal window (6MR), with a diameter of 7.4 Å, thus forming an accessible porous lattice [18].

FAU-X and FAU-Y zeolites have interesting structural and textural properties; for instance, they have a well-controlled pore size distribution, high crystallinity, high thermal, chemical, and mechanical stability, a significant surface area and pore volume, and they are environmentally non-harmful [7,9,14]. Several research papers have reported the excellent adsorption properties of pollutants, such as phosphates, by these zeolites, either used alone or in combination with other adsorbents [15–18]. In addition, the identification of active faujasite sites for adsorption is widely available in several studies [19].

Furthermore, some research studies have attempted to understand the microscopic and macroscopic levels of zeolite adsorption processes using statistical physics models [20]. These models can predict adsorption mechanisms based on physical parameters [21,22], and could be complemented with quantum mechanical calculations based on the DFT to improve the explanation for these materials' adsorption mechanisms [23]. In fact, with the molecular information obtained from the quantum mechanical calculations of an adsorbent material, acidity–reactivity relationships can be formulated to clarify the adsorption mechanism [13]. Therefore, the literature extensively describes the use of DFT simulation in order to understand adsorption phenomena within materials at the molecular level [24–26]. Despite the importance of using DFT simulation to understand the adsorption mechanisms of adsorbent materials, no comparative studies have been found in the literature that use quantum technology to describe the adsorption process of sodium dihydrogen phosphate (SDHP) on FAU-X and FAU-Y zeolites.

The objective of this paper is to contribute to a better understanding of the interaction between SDHP and faujasite-type zeolites; to this end, we present a systematic, theoretical study of the adsorption of this molecule on X- and Y-type faujasite zeolites. Although it is interesting to study the adsorption of different phosphate species, the chosen molecule is the most stable in a neutral pH. The computational results reported in this work—at the molecular level, and by using computational models—attempt to contribute to the understanding of the mechanisms of adsorption of pollutant molecules in wastewater on materials, such as zeolites. This is designed to complement the experimental research that proposes more efficient methods of employing materials with high activity for adsorbing pollutants to solve this environmental problem.

Additionally, a novelty of this study was that the model used was very realistic; it was formed by a 192 XO_4 (X = Si or Al) tetrahedral linked by oxygen atoms, and takes the 760 atoms in the X-faujasite and 630 atoms in the Y-faujasite into account.

2. Materials and Methods

Density Functional Theory (DFT) calculations were performed using the Vienna Ab initio Simulation Package (VASP) code [13,27]. The Density Functional Theory is based on the Hohenberg–Kohn theorems, which proved that the electron density of the ground state contains the information of an electronic system. DFT is widely used to describe the structural and electronic properties of many-body systems, solving Schrödinger's

equation with the Kohn–Sham scheme. In particular, VASP code uses Bloch's theorem to calculate systems with periodic conditions. In this study, the Perdew–Burke–Ernzerhof (PBE) exchange–correlation functional was used for generalized gradient approximation (GGA) [28]. The plane-augmented wave (PAW) method was used to describe the electron–ion interactions [29]. The plane wave cutoff energy was set at 415 eV. The Kohn–Sham equations were solved by a self-consistent field method until the energy difference was lower than 10^{-4} eV. The Brillouin zone integration was sampled using only the Γ-point [30]. The atomic positions were fully relaxed until the forces in each atom were lower than 0.4 eV/Å. Gaussian smearing, with σ = 0.10 eV, was used for the band occupancies and to improve total energy convergence.

A (3 × 3 × 3) cell faujasite supercage was employed as a model; this framework cell was constructed from a cubic cell available in the Materials Studio software, and was later fully optimized. Initially, the cell shape and cell volume of both zeolites models were optimized; then, the atomic positions of the sodium dihydrogen phosphate, of the isolated X- and Y-type faujasite zeolites models, and of the supersystem (adsorbate–zeolite) were fully optimized. The optimized lattice parameters and the volume of the cubic unit cell (96 Si or Al atoms and 384 O atoms) were: a = b = c = 25.028 Å, $\alpha = \beta = \gamma = 90°$, and V = 15.678 $Å^3$. To obtain the FAU-X zeolite model (Si/Al = 1.2), 12 Si atoms were substituted for 12 Al atoms. The negative charge of each of the Al atoms was compensated with a proton (H^+), meaning that 84 H^+ were added to the structure. The resulting molecular formula of the FAU-X zeolite was (H^+) $H_{84}A_{l84}Si_{108}O_{384}$. Similarly, to obtain the FAU-Y zeolite (Si/Al = 2.5), 42 Si atoms were substituted for 42 Al atoms. The negative charge generated by the substitution was compensated by one proton (H^+) so that there were 54 protons in the structure. The resulting molecular formula of the FAU-Y zeolite was $H_{54}Al_{54}Si_{138}O_{384}$. The Al atoms were randomly distributed according to the Lowenstein rule [31]. Figure 1 shows the cubic unit cell of the faujasite zeolite obtained from the Materials Studio software, and Figures 2 and 3 describe the primitive triclinic cell of the FAU-X and FAU-Y zeolites, respectively.

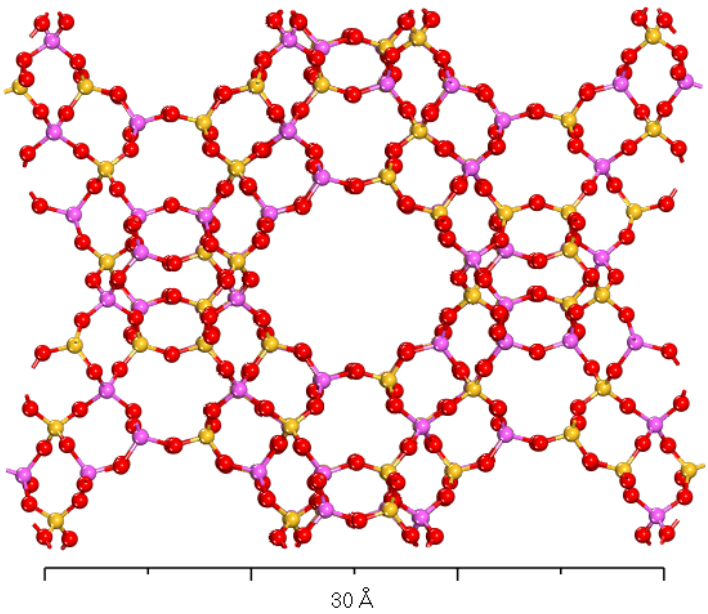

Figure 1. Structural model of the faujasite zeolite obtained from Materials Studio 2017.

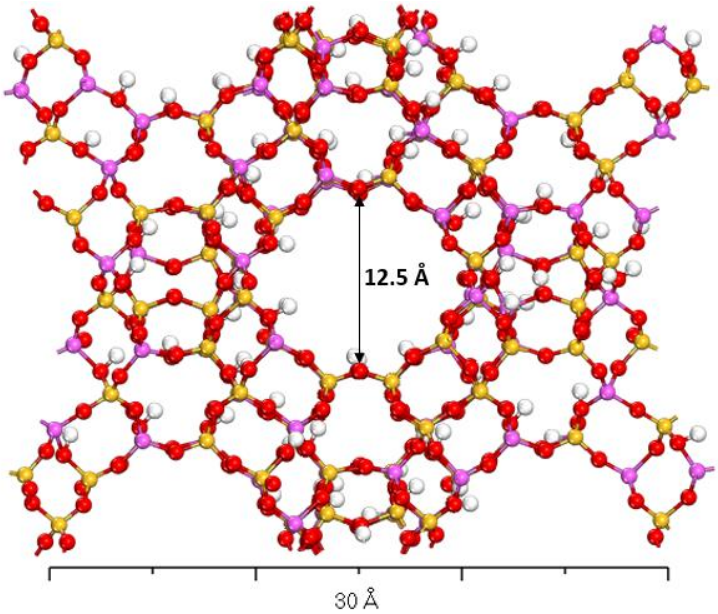

Figure 2. Model of FAU-X: $H_{84}Al_{84}Si_{108}O_{384}$.

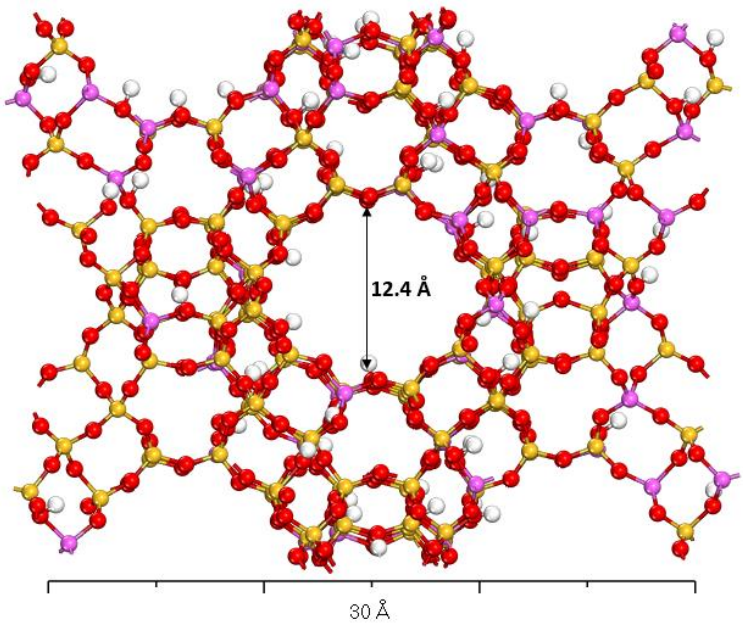

Figure 3. Model of FAU-Y: $H_{54}Al_{54}Si_{138}O_{384}$.

Crystallographic data show that, of the possible acid sites, site II is the most occupied [19,32] and is located in the six rings of the sodalite cage from the supercage side [33]. This site is the most accessible to several adsorbates [34,35], therefore, in this study, site II was considered as an adsorption active site in the SDHP molecule.

Adsorption Energy

The adsorption energy of SDHP on FAU-X and FAU-Y zeolites was calculated using the following Equation [36–38]:

$$\Delta E_{ads} = E_{FAU\text{-}SHDP} - E_{FAU} - E_{SHDP} \quad (1)$$

where:

$E_{FAU\text{-}SHDP}$: The energy of the zeolite molecular supersystem.

E_{FAU}: The energy of the naked zeolite.
E_{SHDP}: The energy of the isolated molecule in vacuum.

3. Results and Discussion

3.1. Molecular Optimization

The P-O bond distances were 1.5 Å and 1.6 Å in the optimized molecular structure of sodium dihydrogen phosphate (NaH_2PO_4), the P-OH bond distance was 1.7 Å, and the O-H bond distance was 1.0 Å. The distance between the Na atom and the P atom was 2.7 Å. The angle formed between the oxygen atoms (121°) was greater than the angles formed by the oxygen atoms that make up the hydroxyl groups (109° and 107°). Figure 4 shows the optimized structure of SDHP.

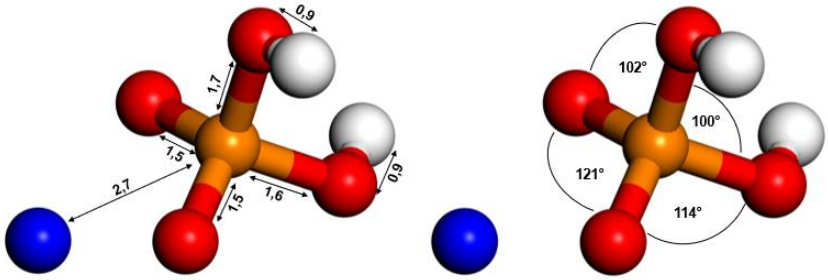

Figure 4. Optimized structural model of the molecule (NaH_2PO_4).

3.2. Optimized X- and Y-Type Faujasite Zeolites

The framework model was a unit cell of approximately 25 Å in each side, and was formed by a 192 XO_4 (X = Si or Al) tetrahedral linked by oxygen atoms, in agreement with bibliographic information [39,40]. The cell parameter and volume before and after a full optimization of the faujasite structure are shown in Table 1. The unit cell of the Y-type faujasite zeolite included 54 Al atoms and 138 Si atoms, and the X-type faujasite zeolite included 84 Al atoms and 108 Si atoms; the optimized cell volume of FAU-X was 15.286 $Å^3$, and that of FAU-Y was 14.975 $Å^3$.

Table 1. Cell parameters before and after full optimization.

Parameter	Faujasite X		Faujasite Y	
	Before	After	Before	After
a (Å)	25.28	24.82	24.83	24.65
b (Å)	25.18	24.83	24.83	24.67
c (Å)	25.16	24.80	24.80	24.63
α (°)	90	89	89	89
β (°)	90	90	90	90
γ (°)	89	89	89	89
V ($Å^3$)	16,012	15,286	15,286	14,975

Therefore, as the Si atoms were substituted for Al atoms, the cell's structure and dimensions were modified. The higher the Si/Al ratio, the more the unit cell's dimensions were increased and the more uniform the structure. Both effects were observed in experimental studies [41,42].

The diameter of the central pore was considered as the length between two oxygen atoms located at opposite extremes of the pore of the optimized framework cell, as shown in Figure 5. The diameter for FAU-X was 12.41 Å, and for FAU-Y it was 12.47 Å; these values were reasonably comparable with experimental data, which indicated that the pore diameters vary between 6 Å and 12 Å [43,44]. An O-H bond distance of 0.97 Å was obtained in the Brønsted acid sites of the optimized zeolite models; this value was very close to the experimental and computational data [45,46].

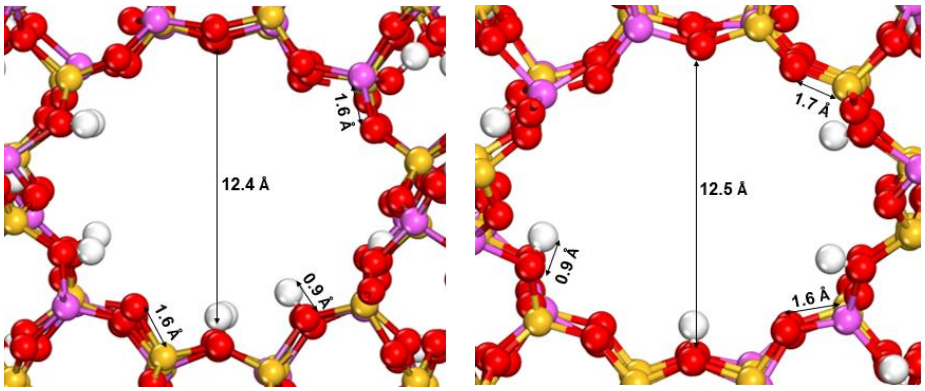

(**a**) (**b**)

Figure 5. Pore diameter and O-H, Si-O, and Al-O distances in FAU-X (**a**) and FAU-Y (**b**) supercages after the optimization process.

The sodalite cages in the faujasite-type zeolites were connected to the tetrahedral through hexagonal prisms. These sodalite units formed so-called β cavities, which were accessible through cavities with a diameter of 2.0 Å to 2.5 Å, and formed by the oxygen atoms of the unshared hexagonal faces [43,47,48]. In the FAU-X structure, the distance between the oxygen atoms of the hexagonal prism was 3.80 Å; likewise, the diameter of the largest sodalite pore was 4.70 Å. The pore dimensions of the FAU-Y structure in the hexagonal prism and the sodalite were 3.7 Å and 5.2 Å, respectively, as shown in Figure 6.

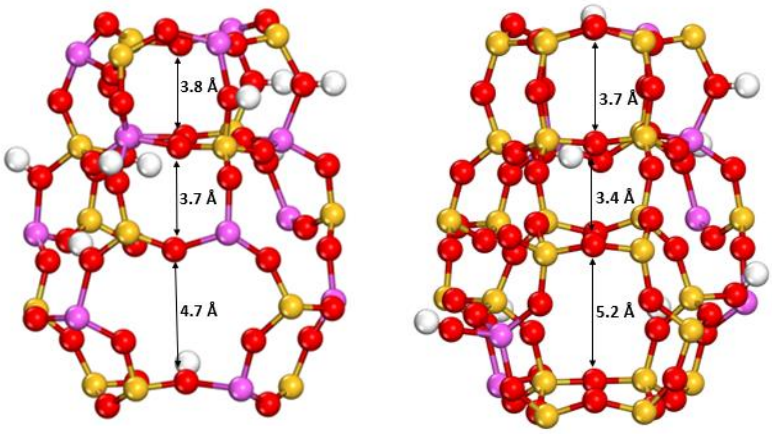

(**a**) (**b**)

Figure 6. Pore diameter in the sodalite cage and hexagonal prism of the optimized FAU-X (**a**) and FAU-Y (**b**) structures.

The Si-O and Al-O bond distances, and Si-O-Si, Si-O-Al, O-Si-O, and O-Al-O bond angles, obtained after the full optimization calculations, are shown in Figure 7. These dimensions were reasonably close to the experimentally reported values.

3.3. Adsorption of Phosphate on X- and Y-Type Faujasites

Two models were used to assess the effect of the substitution of Si atoms for Al atoms on phosphate adsorption activity: a model with a Si/Al ratio of 1.2 for FAU-X, and a model with a Si/Al ratio of 2.5 for FAU-Y. The calculated adsorption energy values for phosphate on both zeolites are shown in Table 3.

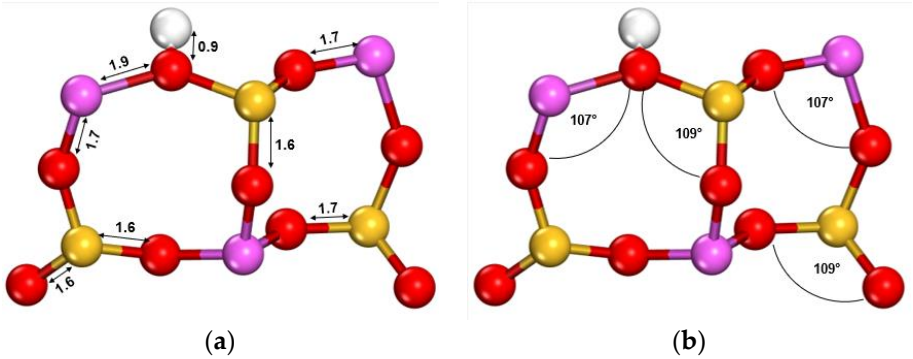

Figure 7. Distance (**a**) and angle (**b**) of the bonds of the FAU-X and FAU-Y optimized framework cells.

Table 2 shows the calculated structural parameters of three computational methods. Experimental X-ray crystallographic data are included [45].

Table 2. Structural parameters using several computational and experimental methods.

Parameter	Method	Si-O	Al-O
Distance (Å)	LDA	1.6	1.7
	NDA	1.7	1.7
	HF-SCF	1.6	1.7
	Experimental	1.6	1.7
	This study	1.6	1.7
Angle (°)		**O-Si-O**	**O-Al-O**
	LDA	110	107
	NDA	110	108
	HF-SCF	109	107
	Experimental	109	109
	This study	109	107

Table 3. Adsorption energy of NaH_2PO_4 on FAU-X and FAU-Y.

Structure	Adsorption Energy			
		eV	kcal/mol	kJ/mol
$E_{FAUX\text{-}FOS}$	Energy of FAUX	−4696.05	—	—
	Energy of the isolated molecule	−44.87	—	—
	Σ (E_{FAUX} + E_{SDHP})	−4740.92		
	Energy of molecule on FAUX	−4741.25	—	—
	Eads	0.33	7.6	32
$E_{FAUY\text{-}FOS}$	Energy of FAUY	−4643.49	—	—
	Energy of the isolated molecule	−44.87	—	—
	Σ (E_{FAUY} + E_{SDHP})	−4688.36		
	Energy of molecule on FAUY	−4690.03	—	—
	Eads	1.67	38.5	161

3.3.1. Adsorption on the FAU-X Model

In the most favored position of the phosphate on FAU-X, with the lowest adsorption energy, the oxygen atoms of the molecule were close to the hydrogen atoms of the pore, forming a bidentate complex, as shown in Figure 8. The bond distance was 1.5 Å. This indicated a possible electrostatic attraction between FAU-X and NaH_2PO_4. This interaction plays an important role in the catalytic activity [49,50].

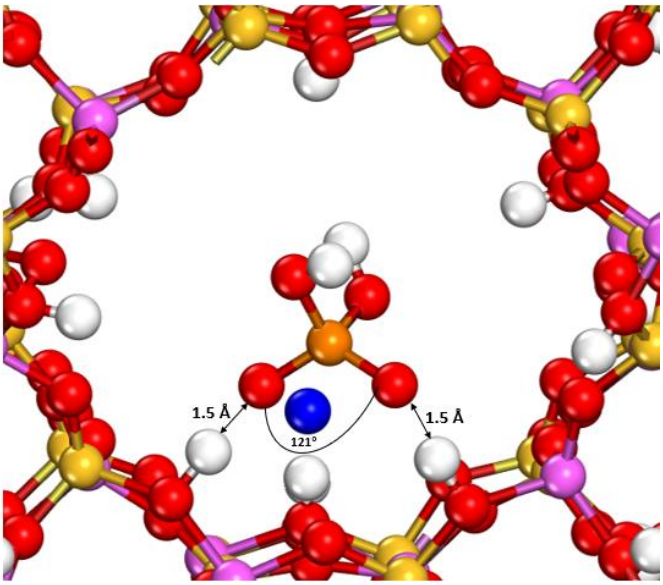

Figure 8. Optimized structure of the shaped system for the adsorbent (FAU-X) and the adsorbate (NaH_2PO_4).

The adsorption energy can be used as a criterion to describe the interaction mechanism between two systems [4]. In this case, an adsorption energy value of 31.64 kJ/mol was obtained, suggesting an exothermic reaction. Similar DFT studies of $H_2PO_4^-$ adsorption as bidentate complexes report an energy of 94.4 kJ/mol at low pH conditions on hydrated Fe oxide [51], and of 22.5 kJ/mol in modified polyether sulfone [1].

Experimentally, it is known that positively charged adsorbents can interact effectively with negatively charged $H_2PO_4^-$ through electrostatic attractions, concluding that, in acidic conditions, phosphate adsorption activity is favored. Adsorption tests in the pH range from 2 to 9 indicate that adsorption activity is greater in the pH range between 4 and 6. In the strongly acidic pH range, phosphate adsorption activity decreases; this could be attributed to the formation of a weak hydrophosphate salt [1,51–54]. In fact, the FAU-X structure is more acidic than FAU-Y, as the latter contains more protons that compensate for the negative charge resulting from the substitution of silicon for aluminum. Therefore, the adsorption energy described for the FAU-X system is different than that for FAU-Y.

It is also known that, at pH values of above 7, there is a reduction in the adsorption of $H_2PO_4^-$, which is attributed to the fact that the surface charge of the adsorbent becomes more negative at higher pH values, causing greater electrostatic repulsion towards the negatively charged phosphate anions [55–58].

3.3.2. Adsorption on FAU-Y Model

The more Si atoms are substituted by Al atoms, the more the protons compensate for the negative charge, therefore, the FAU-Y model has fewer H^+ that compensate for the negative charge generated by the Al atoms in the system. In this case, an oxygen atom of the molecule was placed on a hydrogen atom at site II of the zeolite; this conformation allowed for the placing of two of the hydrogen atoms of the phosphate onto the oxygen atoms of the zeolite model, as shown in Figure 9.

After full optimization, the O(SHDP)-H(FAU-Y) bond distance was 1.4 Å, and the hydrogen atoms of the molecule were located at a distance of 2.3 Å and 2.1 Å, respectively. In addition, the protons of the hydroxyl groups of the molecule interacted with the nearest oxygen atoms of FAU-Y, and one of the oxygen atoms was vertically located on an H atom of this zeolite. Likewise, the O-H bond distance of FAU-Y, closer to the NaH_2PO_4 molecule, was 1.1 Å, which suggested an interaction between an O atom of the NaH_2PO_4 molecule

and an H atom of FAU-Y. A similar computational study of H_3PO_4 adsorption on ZSM-5 showed analogous behavior [3,59].

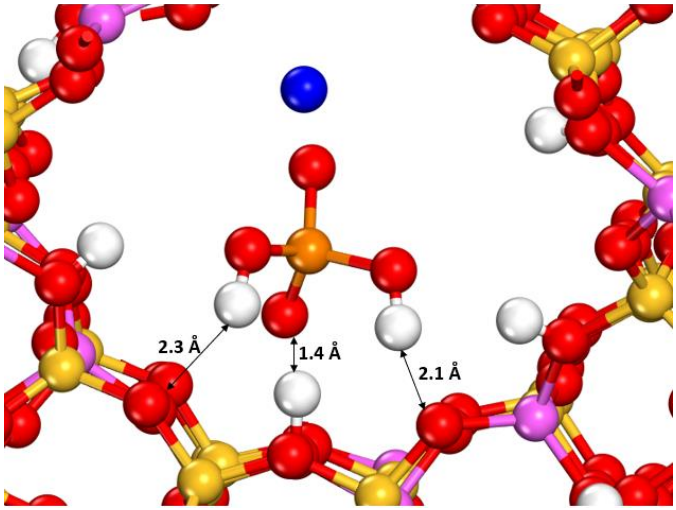

Figure 9. Optimized structure of the shaped system for the adsorbent (FAU-Y) and the adsorbate (NaH_2PO_4).

The hydroxyl groups of sodium dihydrogen phosphate form bonds between the hydrogen atoms and the oxygen atoms of the structure, which act as alkaline sites, and these bonds have an important impact on the stability of the adsorption complexes. In another study, an adsorption energy of 161 kJ/mol was obtained from Mg/Ca-modified biochar structures [4,60]. Furthermore, the adsorption energies of $H_2PO_4^-$ vary in the range of 265.35–317.66 kJ/mol in experiments with hydroxylated alfa-SiO_2 [61].

4. Conclusions

The Y-type faujasite zeolite shows greater activity for the adsorption of NaH_2PO_4 molecules, with an adsorption energy of 161 kJ/mol, compared to the X-type faujasite zeolite system, with an adsorption energy of 31.64 kJ/mol.

Both Brønsted acidic and Lewis alkaline sites favor the adsorption activity of zeolites.

The optimized phosphate molecular structure and unit cell geometrical parameters of the zeolites are in agreement with experimental data.

The terminal hydrogen atoms of zeolites are found at a distance of 0.97 Å from the oxygen atoms. This value increases to 1.1 Å for hydroxides interacting with phosphate. The electrostatic interactions of the phosphate and the oxygen atoms of the zeolite provokes changes in the arrangement of the hydrogen atoms of the molecule.

The supercage or the central pore of zeolites are accessible sites for the interaction of the phosphate molecule.

The corroboration of the obtained computational results with experimental data will be very interesting, as will the complete analysis of all the variables involved in the complex process of decreasing the pollutants of wastewater at the theoretical and experimental level.

This paper only reports the results obtained from dihydrogen phosphate; however, the study of the adsorption of other phosphate species on these models, and also on other adsorbents, is very interesting and promising.

The results of this study contribute to the objective of previous experimental and computational studies that have provided interesting information to improve the understanding of the trapping of phosphates on zeolites as adsorbents.

Author Contributions: Conceptualization, L.F.C.-C., X.J.-F. and S.G.; methodology, L.F.C.-C., X.J.-F. and S.G.; software, L.F.C.-C.; validation, S.G.; investigation, L.F.C.-C., X.J.-F. and S.G.; writing—review and editing, L.F.C.-C., X.J.-F. and S.G.; supervision, S.G. All authors have read and agreed to the published version of the manuscript.

Funding: This research was funded by Universidad Técnica Particular de Loja.

Institutional Review Board Statement: Not applicable.

Informed Consent Statement: Not applicable.

Data Availability Statement: The data presented in this study are available on request from the corresponding author.

Acknowledgments: The authors thank Universidad Técnica Particular de Loja for the support in this study.

Conflicts of Interest: The authors declare no conflict of interest.

References

1. Wang, X.; Song, L.; Yang, F.; He, J. Investigation of phosphate adsorption by a polyethersulfone-type affinity membrane using experimental and DFT methods. *Desalin. Water Treat.* **2016**, *57*, 25036–25056. [CrossRef]
2. Bolaños-Alfaro, J.D.; Cordero-Castro, G.; Segura-Araya, G. Determinación de nitritos, nitratos, sulfatos y fosfatos en agua potable como indicadores de contaminación ocasionada por el hombre, en dos cantones de Alajuela (Costa Rica). *Rev. Tecnol. Marcha* **2017**, *30*, 15. [CrossRef]
3. Huang, W.; Zhang, Y.; Li, D. Adsorptive removal of phosphate from water using mesoporous materials: A review. *J. Environ. Manag.* **2017**, *193*, 470–482. [CrossRef]
4. Yin, Q.; Liu, M.; Li, Y.; Li, H.; Wen, Z. Computational study of phosphate adsorption on Mg/Ca modified biochar structure in aqueous solution. *Chemosphere* **2021**, *269*, 129374. [CrossRef] [PubMed]
5. Islam, M.A.; Morton, D.W.; Johnson, B.B.; Mainali, B.; Angove, M.J. Manganese oxides and their application to metal ion and contaminant removal from wastewater. *J. Water Process Eng.* **2018**, *26*, 264–280. [CrossRef]
6. Currie, S.J.; Van Zomeren, C.M.; Berkowitz, J.F. Utilizing Wetlands for Phosphorus Reduction in Great Lakes Watersheds: A Review of Available Literature Examining Soil Properties and Phosphorus Removal Efficiency. *Environ. Sci.* **2017**.
7. Naranjo, Y. Estudio para mejorar la eliminación de fósforo en humedales artificiales empleando fangos generados en la potabilización del agua, mediante procesos de adsorción. *Microporous Mesoporous Mater.* **2017**, *239*, 111–122.
8. Sierra, N.; Del Peso Díaz, M.I. *Estudio del Proceso de Adsorción de Fosfatos en Hidróxidos Dobles Laminares*; UPM: Madrid, Spain, 2019; pp. 18–25.
9. Gao, Y.; Chen, N.; Hu, W.; Feng, C.; Zhang, B.; Ning, Q.; Xu, B. Phosphate removal from aqueous solution by an effective clay composite material. *J. Solut. Chem.* **2013**, *42*, 691–704. [CrossRef]
10. Bacelo, H.; Pintor, A.M.A.; Santos, S.C.R.; Boaventura, R.A.R.; Botelho, C.M.S. Performance and prospects of different adsorbents for phosphorus uptake and recovery from water. *Chem. Eng. J.* **2020**, *381*, 122566. [CrossRef]
11. Pramanik, B.K.; Islam, A.; Asif, M.B.; Royhand, R.; Pramanik, S.K.; Shah, K.; Bhuiyan, M.; Hai, F. Emerging investigator series: Phosphorus recovery from municipal wastewater by adsorption on steelmaking slag preceding forward osmosis: An integrated process. *Environ. Sci. Water Res. Technol.* **2020**, *6*, 1559–1567. [CrossRef]
12. Guaya, D.; Hermassi, M.; Valderrama, C.; Farran, A.; Cortina, J.L. Recovery of ammonium and phosphate from treated urban wastewater by using potassium clinoptilolite impregnated hydrated metal oxides as N-P-K fertilizer. *J. Environ. Chem. Eng.* **2016**, *4*, 3519–3526. [CrossRef]
13. Losada, L.M.; Bonilla, C.N.; Buitrago, R.C.; Bonilla, J.H.O.; Salamanca, M. Preliminary Study of the Ability of Inorganic Ions Remotion By Synthetic Zeolite Faujasite Type. *Rev. Fac. Cienc. Básicas* **2016**, *11*, 114–123.
14. Cruz, H.I.; Javier, M.S.; Luis, D.I.; Gil, M.D.J.; Pérez, A.D. Remoción De Plomo En Agua a Partir De Material Nanoestructurado, Nanotubos De Carbono Soportados En Zeolita Natural. *Av. Cienc. Ing.* **2017**, *8*, 21–27.
15. Liu, C.; Li, G.; Hensen, E.J.M.; Pidko, E.A. Relationship between acidity and catalytic reactivity of faujasite zeolite: A periodic DFT study. *J. Catal.* **2016**, *344*, 570–577. [CrossRef]
16. Chebbi, M.; Chibani, S.; Paul, J.F.; Cantrel, L.; Badawi, M. Evaluation of volatile iodine trapping in presence of contaminants: A periodic DFT study on cation exchanged-faujasite. *Microporous Mesoporous Mater.* **2017**, *239*, 111–122. [CrossRef]
17. Serrano, D.P.; Escola, J.M.; Pizarro, P. Synthesis strategies in the search for hierarchical zeolites. *Chem. Soc. Rev.* **2013**, *42*, 4004–4035. [CrossRef]
18. Mouni, L.; Belkhiri, L.; Bollinger, J.-C.; Bouzaza, A.; Assadi, A.; Tirri, A.; Dahmoune, F.; Madani, K.; Remini, H. Removal of Methylene Blue from aqueous solutions by adsorption on Kaolin: Kinetic and equilibrium studies. *Appl. Clay Sci.* **2018**, *153*, 38–45. [CrossRef]
19. Kim, D.W.; Han, H.; Kim, H.; Guo, X.; Tsapatsis, M. Preparation of a graphene oxide/faujasite composite adsorbent. *Microporous Mesoporous Mater.* **2018**, *268*, 243–250. [CrossRef]
20. Wongcharee, S.; Aravinthan, V.; Erdei, L. Mesoporous activated carbon-zeolite composite prepared from waste macadamia nut shell and synthetic faujasite. *Chin. J. Chem. Eng.* **2019**, *27*, 226–236. [CrossRef]
21. Setthaya, N.; Chindaprasirt, P.; Yin, S.; Pimraksa, K. TiO2-zeolite photocatalysts made of metakaolin and rice husk ash for removal of methylene blue dye. *Powder Technol.* **2017**, *313*, 417–426. [CrossRef]

22. Sivalingam, S.; Kella, T.; Maharana, M.; Sen, S. Efficient sono-sorptive elimination of methylene blue by fly ash-derived nano-zeolite X: Process optimization, isotherm and kinetic studies. *J. Clean. Prod.* **2019**, *208*, 1241–1254. [CrossRef]
23. Frising, T.; Leflaive, P. Extraframework cation distributions in X and Y faujasite zeolites: A review. *Microporous Mesoporous Mater.* **2008**, *114*, 27–63. [CrossRef]
24. Bouaziz, N.; Manaa, M.B.; Aouaini, F.; Lamine, A.B. Investigation of hydrogen adsorption on zeolites A, X and Y using statistical physics formalism. *Mater. Chem. Phys.* **2019**, *225*, 111–121. [CrossRef]
25. Chiari, L.; Ohnuki, C.; Fujinami, M. A positronium-based systematic study of the physico-chemical properties of zeolite pores. *Radiat. Phys. Chem.* **2021**, *184*, 109441. [CrossRef]
26. Sellaoui, L.; Hseeou, E.P.; Badawi, M.; Netto, M.S.; Dotto, G.L.; Silva, L.F.O.; Tielens, F.; Ifthikar, F.; Bonilla-Petriciolet, A.; Chen, Z. Trapping of Ag^{+}, Cu^{2+}, and Co^{2+} by faujasite zeolite Y: New interpretations of the adsorption mechanism via DFT and statistical modeling investigation. *Chem. Eng. J.* **2020**, 127712. [CrossRef]
27. Ribeiro, R.P.P.L.; Camacho, B.C.R.; Lyubchyk, A.; Esteves, I.A.A.C.; Cruz, F.J.A.L.; Mota, J.P.B. Experimental and computational study of ethane and ethylene adsorption in the MIL-53(Al) metal organic framework. *Microporous Mesoporous Mater.* **2016**, *230*, 154–165. [CrossRef]
28. Piccini, G.; Alessio, M.; Sauer, J.; Zhi, Y.; Liu, Y.; Kolvenbach, R.; Jentys, A.; Lercher, J.A. Accurate adsorption thermodynamics of small alkanes in zeolites. Ab initio theory and experiment for H-chabazite. *J. Phys. Chem. C* **2015**, *119*, 6128–6137. [CrossRef]
29. Sung, C.Y.; al Hashimi, S.; McCormick, A.; Cococcioni, M.; Tsapatsis, M. A DFT study on multivalent cation-exchanged y zeolites as potential selective adsorbent for H2S. *Microporous Mesoporous Mater.* **2013**, *172*, 7–12. [CrossRef]
30. Göltl, F.; Grüneis, A.; Bučko, T.; Hafner, J. Van der Waals interactions between hydrocarbon molecules and zeolites: Periodic calculations at different levels of theory, from density functional theory to the random phase approximation and Moller-Plesset perturbation theory. *J. Chem. Phys.* **2012**, *137*, 114111. [CrossRef]
31. Kresse, G.; Hafner, J. Ab initio molecular dynamics for liquid metals. *Phys. Rev. B* **1993**, *47*, 558–561. [CrossRef]
32. Perdew, J.P.; Burke, K.; Ernzerhof, M. Generalized gradient approximation made simple. *Phys. Rev. Lett.* **1996**, *77*, 3865–3868. [CrossRef]
33. Joubert, D. From ultrasoft pseudopotentials to the projector augmented-wave method. *Phys. Rev. B-Condens. Matter Mater. Phys.* **1999**, *59*, 1758–1775. [CrossRef]
34. Hu, K.; Wu, X.; Hinokuma, S.; Ohto, T.; Wakisaka, M.; Fujita, J.-C.; Ito, Y. Boosting electrochemical water splitting: Via ternary NiMoCo hybrid nanowire arrays. *J. Mater. Chem. A* **2019**, *7*, 2156–2164. [CrossRef]
35. RFletcher, E.; Ling, S.; Slater, B. Violations of Löwenstein's rule in zeolites. *Chem. Sci.* **2017**, *8*, 7483–7491. [CrossRef] [PubMed]
36. Buttefey, S.; Boutin, A.; Mellot-Draznieks, C.; Fuchs, A.H. A simple model for predicting the Na+ distribution in anhydrous NaY and NaX zeolites. *J. Phys. Chem. B* **2001**, *105*, 9569–9575. [CrossRef]
37. Pillai, R.S.; Khan, I.; Titus, E. C2-Hydrocarbon Adsorption in Nano-porous Faujasite: A DFT Study. *Mater. Today Proc.* **2015**, *2*, 436–445. [CrossRef]
38. Nour, Z.; Berthomieu, D.; Yang, Q.; Maurin, G. A computational exploration of the CO adsorption in cation-exchanged faujasites. *J. Phys. Chem. C* **2012**, *116*, 24512–24521. [CrossRef]
39. Arean, C.O.; Delgado, M.R.; Nachtigall, P.; Thang, H.V.; Rubeš, M.; Bulánek, R.; Chlubná-Eliášová, P. Measuring the Brønsted acid strength of zeolites-does it correlate with the O-H frequency shift probed by a weak base? *Phys. Chem. Chem. Phys.* **2014**, *16*, 10129–10141. [CrossRef] [PubMed]
40. Kaduk, J.A.; Faber, J. Crystal Structure of Zeolite Y as a Function of Ino Exchange. *Rigaku J.* **1995**, *12*, 14–34.
41. Verboekend, D.; Nuttens, N.; Locus, R.; Van Aelst, J.; Groen, J.C.; Perez-Ramirez, J.; Sels, B.F. Synthesis, characterisation, and catalytic evaluation of hierarchical faujasite zeolites: Milestones, challenges, and future directions. *Chem. Soc. Rev.* **2016**, *45*, 3331–3352. [CrossRef] [PubMed]
42. Król, M.; Koleżyński, A.; Mozgawa, W. Vibrational Spectra of Zeolite Y as a Function of Ion Exchange. *Molecules* **2021**, *26*, 342. [CrossRef] [PubMed]
43. Giuseppe, G.; Montes, A.; Rodríguez, G. Zeolitas: Características, propiedades y aplicaciones industriales. *Ed. Por. Editor. Innovación Tecnológica* **2000**, *2*, 46–47.
44. Roussel, T.; Didion, A.; Pellenq, R.J.M.; Gadiou, R.; Bichara, C.; Vix-Guterl, C. Experimental and atomistic simulation study of the structural and adsorption properties of faujasite zeolite-templated nanostructured carbon materials. *J. Phys. Chem. C* **2007**, *111*, 15863–15876. [CrossRef]
45. Krishnamurty, S.; Pal, S.; Vetrivel, R.; Chandra, A.K.; Goursot, A.; Fajula, F. The influence of the geometric parameters on the electronic properties of faujasite cluster models as derived from density functional theory and Hartree Fock-self consistent field methods. *J. Mol. Catal. A Chem.* **1998**, *129*, 287–295. [CrossRef]
46. Szyja, B.M.; Smykowski, D.; Szczygieł, J.; Hensen, E.J.M.; Pidko, E.A. A DFT Study of CO2 Hydrogenation on Faujasite-Supported Ir4 Clusters: On the Role of Water for Selectivity Control. *ChemCatChem* **2016**, *8*, 2500–2507. [CrossRef] [PubMed]
47. Gómez Martin, J.M. *Síntesis, Caracterización y Aplicaciones Catalíticas de Zeolitas Básicas*; Universidad Complutense de Madrid: Madrid, Spain, 2001.
48. Davis, M.E.; Lobo, R.F. Zeolite and Molecular Sieve Synthesis. *Chem. Mater.* **1992**, *11*, 756–768. [CrossRef]
49. Huang, Y.; Dong, X.; Li, M.; Zhang, M.; Yu, Y. Density Functional Theory study of the structural and electronic properties of H3PO4/ZSM-5. *RSC Adv.* **2014**, *4*, 14573–14581. [CrossRef]

50. Chaudhury, S.; Varadachari, C.; Ghosh, K. Ab Initio Studies on Hematite Surface and the Adsorption of Phosphate. *J. Theor. Chem.* **2014**, *2014*, 1–7. [CrossRef]
51. Acelas, N.Y.; Mejia, S.M.; Mondragón, F.; Flórez, E. Density functional theory characterization of phosphate and sulfate adsorption on Fe-(hydr)oxide: Reactivity, pH effect, estimation of Gibbs free energies, and topological analysis of hydrogen bonds. *Comput. Theor. Chem.* **2013**, *1005*, 16–24. [CrossRef]
52. Ning, P.; Bart, H.J.; Li, B.; Lu, X.; Zhang, Y. Phosphate removal from wastewater by model-La(III) zeolite adsorbents. *J. Environ. Sci.* **2008**, *20*, 670–674. [CrossRef]
53. Landers, J.; Gor, G.Y.; Neimark, A.V. Density functional theory methods for characterization of porous materials. Colloids Surfaces A Physicochem. *Eng. Asp.* **2013**, *437*, 3–32. [CrossRef]
54. Mir, J.M.; Mir, M.A.; Majid, S.A. Molecular electron density and nitrate-phosphate sorption efficiency of zeolite-A: Physico-chemical and DFT analyses. *Indian J. Chem.-Sect. A* **2020**, *59*, 939–947.
55. Islam, M.A.; Morton, D.W.; Johnson, B.B.; Pramanik, B.K.; Mainali, B.; Angove, M.J. Metal ion and contaminant sorption onto aluminium oxide-based materials: A review and future research. *J. Environ. Chem. Eng.* **2018**, *6*, 6853–6869. [CrossRef]
56. Zhang, L.; Zhou, Q.; Liu, J.; Chang, N.; Wan, L.; Chen, J. Phosphate adsorption on lanthanum hydroxide-doped activated carbon fiber. *Chem. Eng. J.* **2012**, *185*, 160–167. [CrossRef]
57. Yaguchi, M.; Uchida, T.; Motobayashi, K.; Osawa, M. Speciation of Adsorbed Phosphate at Gold Electrodes: A Combined Surface-Enhanced Infrared Absorption Spectroscopy and DFT Study. *J. Phys. Chem. Lett.* **2016**, *7*, 3097–3102. [CrossRef]
58. Li, X.; Kuang, Y.; Chen, J.; Wu, D. Competitive adsorption of phosphate and dissolved organic carbon on lanthanum modified zeolite. *J. Colloid Interface Sci.* **2020**, *574*, 197–206. [CrossRef]
59. Loayza, L.; Guaya, D. Phosphate Sequestration From Aqueous Solutions Using A Zeolite in The Zinc Form. *Res. Sq.* **2020**, *4*, 10–12. [CrossRef]
60. Kubicki, J.D.; Paul, K.W.; Kabalan, L.; Zhu, Q.; Mrozik, M.K.; Aryanpour, M.; Pierre-Louis, A.-M.; Strongin, D.R. ATR-FTIR and density functional theory study of the structures, energetics, and vibrational spectra of phosphate adsorbed onto goethite. *Langmuir* **2012**, *28*, 14573–14587. [CrossRef] [PubMed]
61. Ji, W.; Tang, Q.; Shen, Z.; Fan, M.; Li, F. The adsorption of phosphate on hydroxylated alpha-SiO_2 (0 0 1) surface and influence of typical anions: A theoretical study. *Appl. Surf. Sci.* **2020**, *501*, 144233. [CrossRef]